JCB Article

SadA, a novel adhesion receptor in *Dictyostelium*

Petra Fey,[1] Stephen Stephens,[2] Margaret A. Titus,[2] and Rex L. Chisholm[1]

[1]Department of Cell and Molecular Biology, Northwestern University Medical School, Chicago, IL 60611
[2]Department of Genetics, Cell Biology, and Development, University of Minnesota, Minneapolis, MN 55455

Little is known about cell–substrate adhesion and how motile and adhesive forces work together in moving cells. The ability to rapidly screen a large number of insertional mutants prompted us to perform a genetic screen in *Dictyostelium* to isolate adhesion-deficient mutants. The resulting substrate adhesion–deficient (sad) mutants grew in plastic dishes without attaching to the substrate. The cells were often larger than their wild-type parents and displayed a rough surface with many apparent blebs. One of these mutants, sadA$^-$, completely lacked substrate adhesion in growth medium. The sadA$^-$ mutant also showed slightly impaired cytokinesis, an aberrant F-actin organization, and a phagocytosis defect. Deletion of the *sad*A gene by homologous recombination recreated the original mutant phenotype. Expression of sadA–GFP in sadA-null cells restored the wild-type phenotype. In sadA–GFP-rescued mutant cells, sadA–GFP localized to the cell surface, appropriate for an adhesion molecule. SadA contains nine putative transmembrane domains and three conserved EGF-like repeats in a predicted extracellular domain. The EGF repeats are similar to corresponding regions in proteins known to be involved in adhesion, such as tenascins and integrins. Our data combined suggest that sadA is the first substrate adhesion receptor to be identified in *Dictyostelium*.

Introduction

Cell–substrate adhesion is a major aspect of amoeboid movement in the social amoeba *Dictyostelium discoideum* as well as in certain mammalian blood and tumor cells. Amoeboid crawling is marked by high membrane turnover rates (Aguado-Velasco and Bretscher, 1999), which would be opposed by strong attachment mediated by focal adhesions or focal contacts (for review see Friedl et al., 2001). Although this explains why focal adhesion complexes have not been identified in *Dictyostelium*, it is likely that molecules exist that are responsible for cell–substrate adhesion in rapidly crawling cells.

Dictyostelium is a single cellular organism that lives in the soil, feeds on bacteria, and divides every 6–8 h. In nature, the amoebae attach to many diverse substrates. When the food source becomes exhausted, cells stop dividing and develop into a multicellular fruiting body. Early on, this involves chemotaxis and aggregation, and much attention has been given to chemotactic signaling, pseudopod extension, and locomotion. Interactions with the underlying substrate during attachment have received much less attention and remain to be defined.

Several proteins that mediate cell–cell adhesion during specific stages of *Dictyostelium* development have been identified. The two major types of cell–cell adhesion are represented by EDTA-sensitive and EDTA-resistant cell–cell contacts. During the initiation of development, DdCad-1 (gp24), a small, secreted glycoprotein with similarities to vertebrate cadherins, mediates EDTA-sensitive cell–cell adhesion (Brar and Siu, 1993; Wong et al., 1996). At the onset of aggregation, expression of gp80/contact sites A (csA) leads to EDTA-resistant cell–cell adhesion (Siu et al., 1985). However, in contact sites A (csA)–null cells, substrate adhesiveness is increased and migration delayed, suggesting also a "de-adhesion" function (Ponte et al., 1998). In the post-aggregation stage, gp150 mediates EDTA-resistant cell–cell adhesion (Gao et al., 1992; Wang et al., 2000). Upon starvation, another developmentally regulated adhesion molecule, ampA, is secreted. This protein is thought to function as an anti-adhesive to limit cell–cell and cell–substrate adhesion during development (Varney et al., 2002). To date, none of these molecules have been directly implicated in binding to substrate, and neither integrin homologues nor other adhesion receptors have been identified.

A few molecules in *Dictyostelium* have been characterized that do play a role in cell–substrate adhesion. Talin is a protein that links the plasma membrane to the cytoskeleton (Burridge and Connell, 1983). Talin binds actin (Muguruma et al., 1990) and vinculin (Burridge and Mangeat, 1984), and has been shown to assemble into focal adhesions via β integrin

The online version of this article includes supplemental material.

Address correspondence to Rex L. Chisholm, Department of Cell and Molecular Biology, Northwestern University Medical School, 303 E. Chicago Ave., Chicago, IL 60611. Tel.: (312) 503-4151. Fax: (312) 503-5994. E-mail: r-chisholm@northwestern.edu

Key words: *Dictyostelium*; cell–substrate adhesion; EGF-like repeats; phagocytosis; cytokinesis

The Journal of Cell Biology, Volume 159, Number 6, December 23, 2002 1109–1119
http://www.jcb.org/cgi/doi/10.1083/jcb.200206067

binding (Horwitz et al., 1986; Knezevic et al., 1996; Moulder et al., 1996). A full-length talin homologue has been identified in *Dictyostelium* (Kreitmeier et al., 1995), and talin-null cells were found to be defective in phagocytosis and adhesion (Niewohner et al., 1997). A myosin VII mutant, created to investigate myosin VII's role in phagocytosis, has deficiencies in cell–cell as well as cell–substrate adhesion (Titus, 1999; Tuxworth et al., 2001). Another protein discovered in a screen for phagocytosis mutants is phg1, a putative nine-transmembrane protein implicated in adhesion to phagocytic and surface substrates (Cornillon et al., 2000). The small GTPase rasG has been suggested to control the actin cytoskeleton (Tuxworth et al., 1997) and to be involved in adhesion; cells that constitutively express the activated form of rasG have been reported to show increased substrate adhesion (Chen and Katz, 2000). Although these molecules have been shown to play a role in adhesion, none of the affected mutants demonstrate a severe loss of cell–substrate adhesion. It also remains unclear if, or how, the proteins would interact. Thus, major players in substrate adhesion must still be identified.

To identify genes important for substrate adhesion in *Dictyostelium*, we performed an insertional mutagenesis screen using restriction enzyme–mediated integration (REMI;* Kuspa and Loomis, 1992). After mutagenesis, we selected for transformants that lost their ability to adhere to the surface of a plastic dish by repeatedly transferring nonattached cells to new dishes, effectively throwing away cells still able to attach. Here we describe the screen and characterize one of the isolated mutants, in which the affected gene encodes a novel, putative adhesion receptor, sadA.

Results

The REMI screen

Because little is known about cell–substrate adhesion in *Dictyostelium* and other amoeboid cells, we performed a REMI screen to isolate mutants that lost their ability to adhere to the underlying substrate. A total of ~72,000 transformants were screened by physically separating nonattached from attached cells. This resulted in the isolation of amoebae that floated when grown in a plastic dish and were largely unable to attach. To date, this screen has identified nine different substrate adhesion genes with multiple isolates for two of them. Adhesion assays indicate that two of the nine mutants show limited ability to adhere to substrate, whereas the others are essentially unable to attach to plastic in HL-5 medium. The affected genes of seven mutants contain predicted membrane spanning domains, suggesting that they encode transmembrane proteins, a characteristic consistent with a role in substrate adhesion.

SadA is a putative nine-transmembrane protein

We have focused our attention on one mutant, 3IIG11, from which we cloned 300 bps of DNA flanking the site of plasmid insertion. When subjected to a blast search of the available *Dictyostelium* genome sequence, this fragment matched a portion of contig 15235 (http://www.sanger.ac.uk/cgi-bin/blast/getseq?db=dictypub/contigs;acc=Contig15235). This contig contained a 2,790-bp genomic DNA sequence and was found to span most of the gene we have named sadA, for substrate adhesion deficient. This sequence contained 340 bp of 5′ untranslated DNA and three exons separated by short introns. In mutant 3IIG11, the plasmid inserted into a DpnI site just upstream of the first intron, 615 bp downstream of the initiation codon. This was confirmed by PCR. Because there was no stop codon in the third exon revealed by the contig, it seemed likely that the gene extended beyond the end of the contig. A full-length sadA cDNA was then cloned from a cDNA library (Robinson and Spudich, 2000). Based on this cDNA and the genomic information, the sadA gene appears to consist of three exons, 626 bp, 585 bp, and 1645 bp long, coding for 952 amino acids. To confirm that the plasmid insertion caused the adhesion-deficient phenotype,

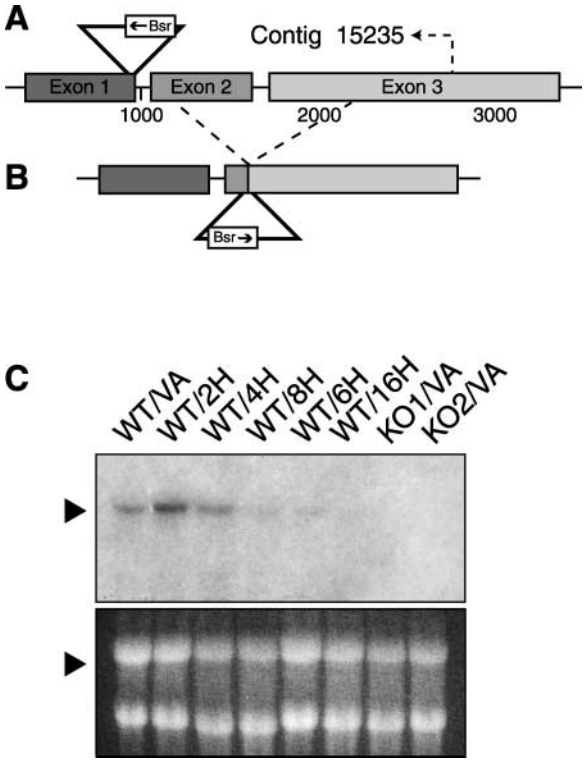

Figure 1. **SadA locus and transcript.** (A) SadA gene structure and plasmid insertion site. In REMI mutant 3IIG11, the transforming plasmid pUCΔBamBsr inserted at the 3′ end of the first exon, disrupting transcription of the remainder of the gene. Indicated at position 2790 is where the sequence of contig 15235 ends. (B) Structure of the knock-out construct. The plasmid pUCΔBamBsr containing genomic flanking sequences was inserted by homologous recombination so that the vector inserted in opposite direction as compared with the initial REMI mutant and resulted in the deletion of a 1-kb genomic sequence. (C) Northern blot analysis. In vegetative wild-type cells (WT/VA), the sadA transcript is ~3.5 kb long. The presence of the transcript in developing wild type was tested after 2, 4, 6, 8, and 16 h starvation. Note that the gene is significantly down-regulated after 4 h starvation. The sadA transcript is absent in vegetative amoebae of two independent knock-out strains (KO1/VA and KO2/VA). As a loading control, the ethidium bromide–stained gel is shown.

*Abbreviation used in this paper: REMI, restriction enzyme–mediated integration.

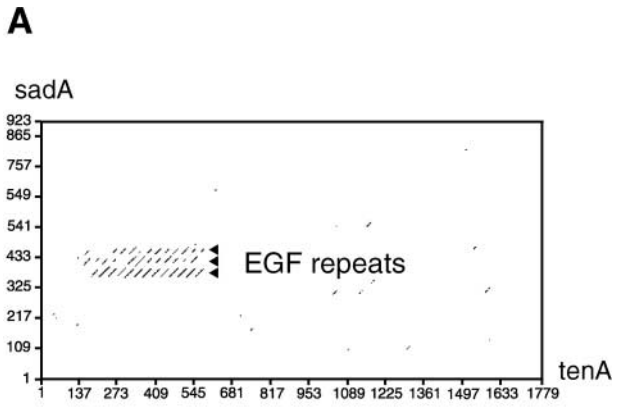

Figure 2. **Similarity of sadA to tenascin A (chicken) and predicted protein organization.** (A) The dot matrix alignment illustrates the high similarity of sadA's three and tenascin A's 13.5 EGF-like repeats. There is virtually no similarity outside this region. The dot matrix plot was created by the Vector NTI Suite 6 (Informax Inc.), using a window size of 30 amino acids and a stringency of 30%. (B) According to the prediction of the TMHMM V2.0 computer program, nine transmembrane regions are depicted. The 25 amino acids predicted to be a signal peptide (SignalP V1.1) were omitted in this model. Each EGF-like repeat comprises six conserved cysteines (black dot) and one conserved glycine residue (dark gray dot).

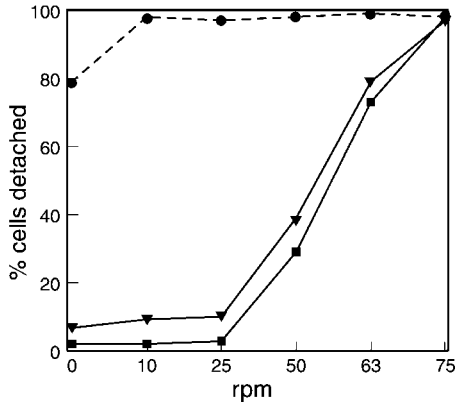

Figure 3. **SadA-null cells cannot initiate attachment.** Cells were plated at 10^5 per ml, grown overnight, and subjected to rotation on an orbital shaker. Subsequently, cells floating in the medium were counted. In the 0-rpm data, the number of detached cells was determined without prior agitation. Here, because most sadA-null cells (closed circles) sank to the surface by gravity overnight, recovery was only ~80%, not close to 100%, although the cells were generally not attached. In all other samples, the detached cells were counted after they were subjected to shear stress from 10 to 75 rpm for 1 h. After agitation at any speed, nearly all sadA-null cells were in the supernatant. In comparison, even at 50 rpm, 71% of wild-type cells (closed squares), and 61% of sadA–GFP-rescued cells (closed inverted triangles) remained attached. Only vigorous shaking at 75 rpm detached all wild-type and rescued cells.

we targeted the sadA gene with an independent targeting construct, which efficiently disrupted the gene in wild-type cells. This resulted in the deletion of an ~1-kb genomic sequence (890 bp coding) (Fig. 1 B). While the sadA transcript in wild-type cells is ~3.5 kb, it is absent in the sadA knockout (Fig. 1 C). These cells showed the same adhesion defect as was observed in the original REMI mutant. All subsequent analyses were done with this mutant (sadA null).

The predicted molecular mass of the 952–amino acid sadA protein is 104.7 kD. A blast search against GenBank/EMBL/DDBJ did not identify strong similarities to any known proteins except for the region between residues 376 and 506, where sadA is 43% identical and 51% similar to the extra-cellular matrix protein tenascin A from chicken. SadA contains three EGF-like repeats in this region, each containing six conserved cysteines with the consensus x(4)-C–x(3,5)–C–x(5,7)–C–x(4,6)–C-x-C-x(5)-G-x(2)-C. Fig. 2 A shows a dot matrix alignment of sadA and tenascin A. The plot shows that the similarity is limited to the region of sadA's three EGF domains that align with tenascin A's 13.5 EGF-like repeats. This conserved part of sadA also has similarity to β integrins and other EGF domain–containing proteins. A common feature of EGF repeats is that they are found in the extracellular domain of membrane-bound proteins. Interestingly, the computer program TMHMM V2.0 (Krogh et al., 2001), which recently was rated the best transmembrane prediction program (Moller et al., 2001), predicted that sadA contains nine transmembrane domains oriented to place the EGF-like repeats in an extracellular domain. The protein is also predicted to contain a signal sequence, likely to be cleaved after residue 25. A model of the protein structure is depicted in Fig. 2 B.

SadA is required for cell attachment and other related processes

When grown in a Petri dish, some sadA-null cells settle on the surface by gravity, but show no signs of either attachment or spreading. To quantitatively assess attachment, we determined the percentage of unattached cells. Cells were grown in plastic dishes for 1 d and then were subjected to

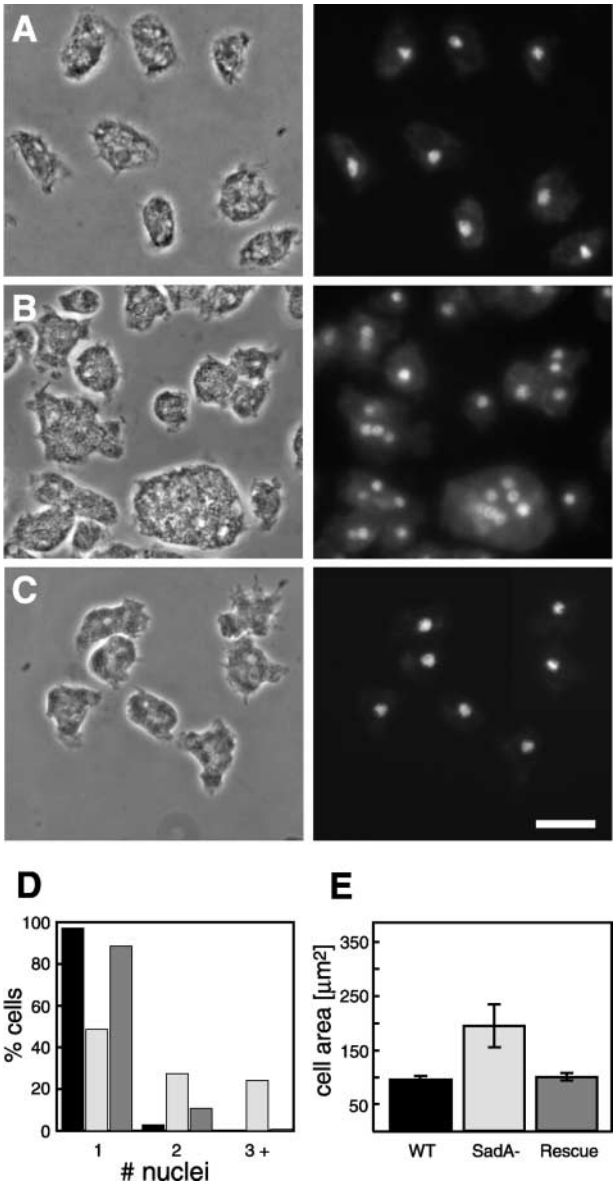

Figure 4. **SadA-null cells are generally larger and multinucleate.** (A) Wild-type AX3, (B) sadA-null, and (C) sadA–GFP-rescued cells. Cells were flattened under an agarose sheet before fixation. Note the correlation of cell size and nuclei number. Bar, 10 μm. (D) A graph illustrating the nuclei number of wild type (black bar), sadA null (light gray), and sadA–GFP rescue (dark gray). For each cell type, the nuclei of 200 cells were counted. (E) A graph illustrating the cell surface area. 12 fixed and flattened cells were measured for each cell type.

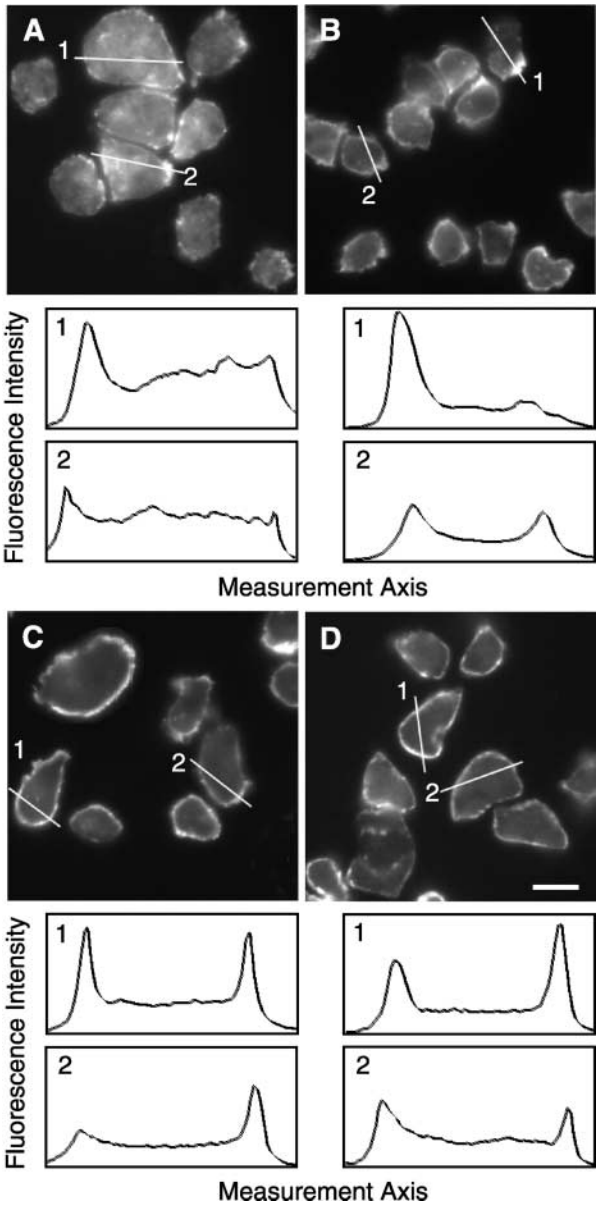

Figure 5. **F-actin is mislocalized in vegetative and indistuinguishable from wild type in starved cells.** Actin was stained with Alexa®568, and actin intensity profiles were created from cross sections of two cells each. (A) Vegetative sadA-null cells. (B) Vegetative wild-type cells. (C) 4-h developed sadA-null cells. (D) 4-h developed wild-type cells. Note that after 4 h starvation, wild-type and mutant cells are indistinguishable. Bar, 10 μm.

rotation on an orbital shaker at various speeds. After 1 h, unattached cells were counted. As the graph in Fig. 3 shows, 70% of wild-type cells stayed attached when shaken at 50 rpm, whereas sadA-null cells were not able to initiate attachment, even in the absence of shaking (0 rpm).

Although the size of wild-type cells grown in Petri dishes is fairly uniform (averaging 10 μm), in mutant cells, there was much more variation in size. Visible especially when flattened and fixed, some of the mutant cells were substantially bigger than wild-type cells (Fig. 4 E). Therefore we stained the nuclear DNA with DAPI to assess the number of nuclei in the cells. A majority of the mutant cells (52%) had two or more nuclei, indicating a cytokinesis defect (Fig. 4, A–D).

A possible explanation for the adhesion and cytokinesis defects and overall appearance could be defects in the cytoskeleton. When we stained the microtubule networks, we found no major differences with wild type, especially when mononucleate cells were compared. Even in multinucleate sadA-null cells, we found a microtubule organizing center and normal-appearing microtubule arrays associated with each nucleus (unpublished data). F-actin in vegetative wild-type amoebae was predominantly located in the cortex with an accumula-

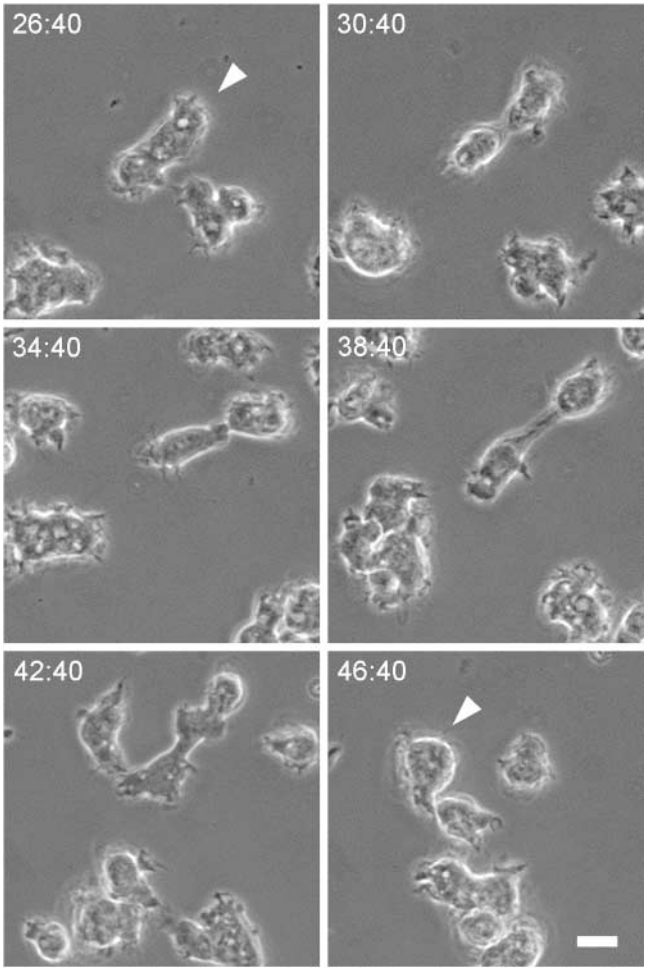

Figure 6. **Axenically growing sadA-null cells.** A cell going through an unsuccessful attempt to divide is marked by an arrow. The cell tried to pull apart, but finally "snapped" back together. Note that the whole process took more than 20 min, whereas a cell division in wild type is typically completed in 6–8 min. Note also that the cells display blebs and are neither attached nor spread (visible in the high refractive index of the light around the edges of the cells). For a better impression of the behavior of growing sadA-null cells, including the division of big cells into many daughters, and for a direct comparison with wild type, see the time-lapse videos (Videos 1 and 2, available online at http://www.jcb.org/cgi/content/full/jcb.200206067/DC1). Bar 10 μm.

tion in pseudopods and a low, but uniform, distribution in the cytoplasm (Fig. 5 B). In contrast, sadA-null amoebae may have also accumulated F-actin in the cortex, but with a less continuous and more punctuate distribution. Moreover, there was significantly more F-actin in the cytoplasm, often in aggregates (Fig. 5 A). After 4 h starvation, however, F-actin localization became exclusively cortical in both wild-type and mutant cells, at which point the two cell types were basically indistinguishable (Fig. 5, C and D). These results suggest that sadA plays a role in the organization of the actin cytoskeleton in vegetative cells, but not after the onset of development.

In a Petri dish, cells remain suspended, have a blebby appearance, never spread, and often fail to divide. Although sadA-null cells grew suspended above the plate, they divided more frequently than wild type. Failed divisions were observed in wild type–sized mutant cells (Fig. 6; Video 1, available online at http://www.jcb.org/cgi/content/full/jcb.200206067/DC1), whereas multinucleate cells often divided into many small daughter cells simultaneously (Video 1). Overall, this resulted in more cell divisions in a given time period than in wild type. When we measured growth rates in suspension, we found that sadA-null cells, despite their apparent cytokinesis defect, had a shorter doubling time (10.2 h) than wild type (12 h) (Fig. 7 A). This suggests that in sadA cells, the division of multinucleate cells into many daughters more than compensates for the cytokinesis defect observed in smaller cells.

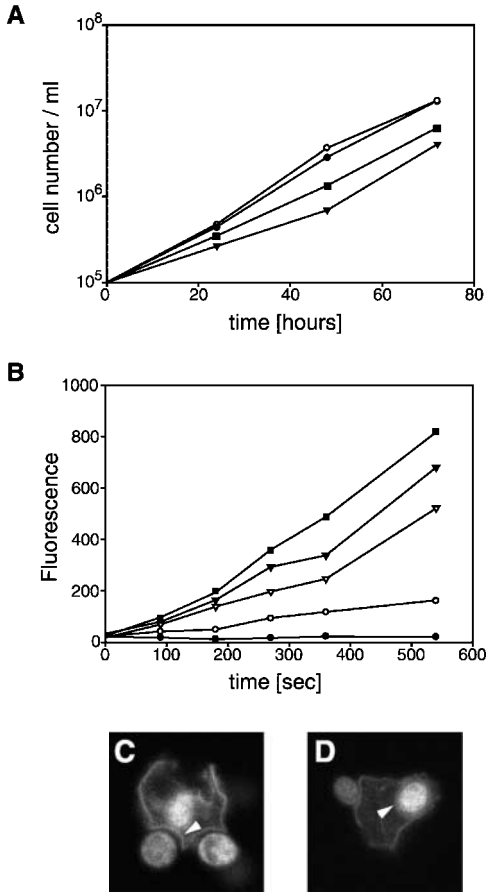

Figure 7. **Growth and phagocytosis of sadA-null cells.** (A) SadA-null cells grow faster in suspension. Two independent sadA-null strains (KO1 and KO2, open and closed inverted triangles, respectively) grow faster than wild type (open circles) and sadA–GFP-rescued mutant cells (closed circles). Doubling times were 10.1, 10.2, 12, and 13.5 h, respectively. After cells were established in suspension, growth was monitored for 3 d. (B) SadA-null cells have a strong phagocytosis defect. Cells were tested for the uptake rate of fluorescent latex beads over the course of 9 min. In sadA-null cells (closed circles), the uptake of beads was completely abolished. SadA–GFP-rescued mutant cells were sorted into high- (closed inverted triangles) and low-expressing (open inverted triangles) cells. In comparison to wild type (open circles), the low-expressing cells rescued the phagocytosis phenotype 64%, whereas the high-expressing cells showed an 83% rescue. For comparison, in myosin VII–null cells (closed squares), phagocytosis is reduced by ~80% (see Discussion). (C and D) SadA is localized, but not enriched, in the phagocytic cup. SadA–GFP-rescued cells during an early (C) and later (D) stage of phagocytosis of heat-killed yeast particles (which show some autofluorescence).

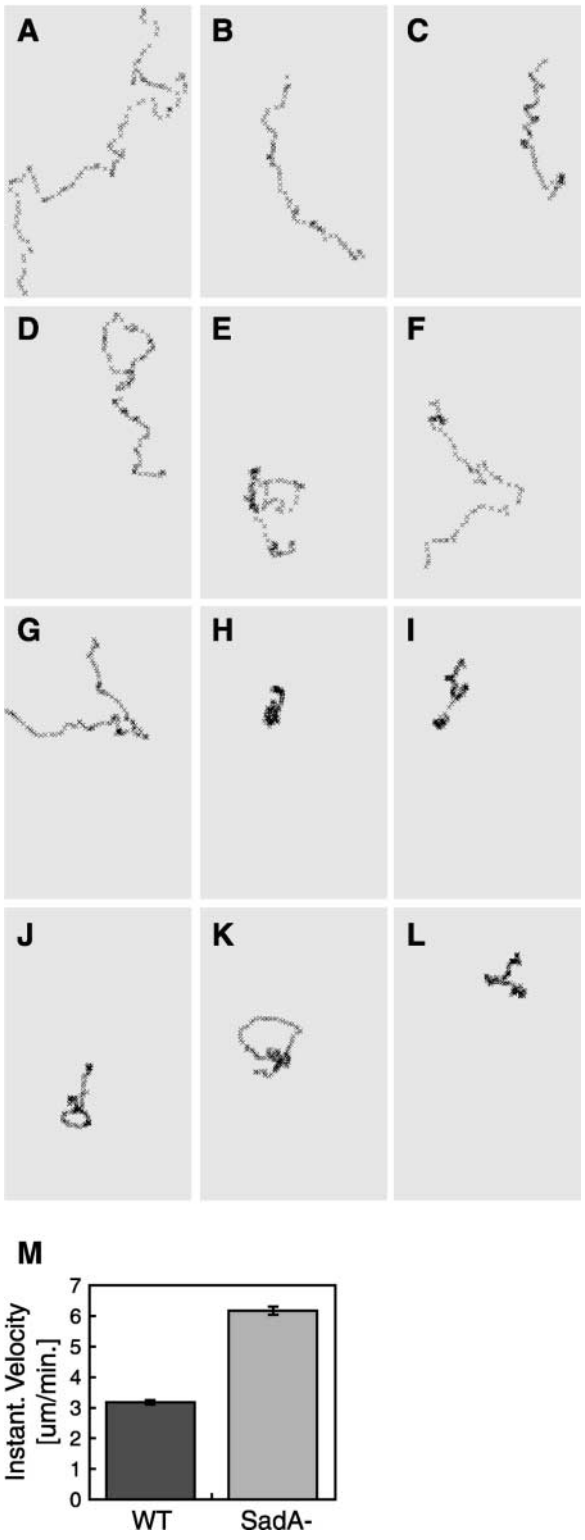

Figure 8. **Vegetative sadA cells move faster than wild type.** Following the paths of growing cells shows that sadA-null cells (A–F) move relatively fast (6.3 μm/min) (M), whereas wild-type cells (G–L) migrate with greater path persistence, at a slower rate (3.2 μm/min) (M). Six cells, shown in Videos 1 (sadA mutant) and 2 (wild type), available at http://www.jcb.org/cgi/content/full/jcb.200206067/DC1, were tracked.

When grown on bacteria on agar plates, sadA-null cells showed plaque sizes only half that of wild type 3 d after plating. This could be the result of slower cell motility or inefficient bacterial uptake. To further investigate the basis of the small plaque size, we assayed phagocytosis of latex beads in phosphate buffer suspension. As illustrated in Fig. 7 B, in sadA-null cells, phagocytosis of beads was completely abolished. The absence of bead uptake suggests that sadA is involved in the initial steps of phagocytosis.

SadA plays a role in the motility of vegetative, but not developing, cells

We measured the instantaneous velocities of growing cells. All wild-type cells typically stayed in the field of vision over long periods of time and smoothly moved short distances with great path persistence. SadA-null cells, in contrast, moved over much larger distances, often clumping with other cells and floating out of the field of view; only a few cells could be followed over longer time periods. The average instantaneous velocities were 3.2 μm/min for vegetative wild-type cells, and almost double, 6.3 μm/min, for mutant cells (Fig. 8). During development, however, when we observed streaming cells (see Videos 3 and 4, available online at http://www.jcb.org/cgi/content/full/jcb.200206067/DC1) or measured the direct response to cAMP in a spatial gradient using a Zigmond chamber (unpublished data), we found no difference between wild-type and mutant behavior. Mutant cells were able to polarize and migrate at normal velocities, comparable to wild type, at around 12 μm/min. Further development into fruiting bodies was also normal (unpublished data). These results show that the sadA adhesion molecule plays an important role in vegetative, but not developing, cells. These data are consistent with our Northern blot results, showing very little sadA expression after the 4-h developmental stage (Fig. 1 C), and with our developmental studies of F-actin localization.

SadA–GFP localizes to the cell cortex and rescues the deletion phenotype

Expression of a sadA–GFP fusion construct in the sadA-null background allowed us to investigate sadA localization. Fluorescence microscopy showed that sadA–GFP localized to the cell cortex (Fig. 9). When we analyzed sadA–GFP-expressing cells by confocal microscopy, we found that sadA localized uniformly throughout the cell surface, and not just to the region of the membrane in contact with the substrate (unpublished data). This result supports the idea that sadA, although not locally restricted, is a transmembrane protein.

Introduction of sadA–GFP into sadA-null cells rescued the mutant phenotypes. When grown in a Petri dish, ~95% of the rescued cells attach (nearly the wild-type rate). Attachment maintenance was also comparable to wild type, with 60% of the sadA-rescued mutant cells still attached at 50 rpm (Fig. 3). Observation of live cells showed that the rescued cells are able to attach and spread, indistinguishably from wild type (unpublished data). DAPI staining showed slightly more bi-nucleate sadA-rescued cells than wild type (10% vs. 2%), however, the vast majority of sadA–GFP-expressing cells was mononucleate

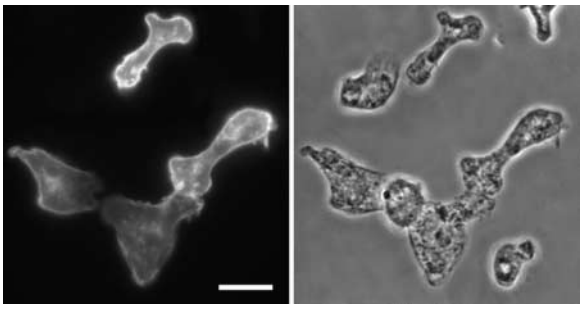

Figure 9. **SadA is predominantly localized in the cortex.** Fixed sadA–GFP-rescued mutant cells in transmitted and fluorescent light are shown. Note the different expression levels of sadA–GFP and that in some cells expression is very low or undetectable. Bar, 10 μm.

like wild-type cells (Fig. 4). This indicates that sadA–GFP rescues the cytokinesis defect seen in sadA mutants. The growth rate in suspension was also restored to nearly wild-type rates by expression of sadA–GFP.

When we tested the phagocytosis rates of sadA–GFP-expressing sadA-null cells we found a partial rescue (75%) of bead uptake. To determine if the phagocytosis efficiency of sadA–GFP-rescued cells depends on expression levels, cells were FACS® sorted based on their levels of GFP fluorescence, and phagocytosis assays were performed on the 10% brightest and 10% dimmest cells (Fig. 9, compare expression levels). Fig. 7 B shows that cells expressing higher levels of sadA–GFP have a phagocytosis rate approaching wild type (83%), whereas the low-expressing cells showed phagocytosis rates somewhat lower (64%) than the whole population of sadA–GFP cells (unpublished data). Thus, sadA–GFP expression significantly rescues the phagocytosis defect and this rescue depends on sadA–GFP expression levels. SadA localized to the phagocytic cup throughout phagocytosis, although there seemed to be no significant enrichment relative to its overall cortical distribution (Fig. 7, C and D).

Discussion

A genetic screen successfully identified substrate adhesion mutants

Using axenically grown *Dictyostelium* amoebae, we performed a genetic screen to identify molecules, and help define biochemical pathways, that mediate cell–substrate adhesion. We screened 72,000 transformants and identified nine independent adhesion mutants where the mutagenizing DNA inserted into different genes. This validates the approach used in this screen and demonstrates that a significant number of genes are required for cell–substrate adhesion in vegetative *Dictyostelium* amoebae.

Detailed analysis of one of these mutants revealed that the transformed plasmid inserted into the coding region of a novel gene, *sad*A. In addition to the strong substrate-adhesion deficiency, sadA-null mutants show a blebby appearance, a wide range of cell sizes reflecting a cytokinesis defect, an increased suspension growth rate, mislocalized F-actin, and a severe phagocytosis defect. Deletion of the *sad*A gene in wild-type cells by gene targeting produced the same collection of phenotypes, which were rescued by introduction of GFP-tagged sadA into sadA knock-out cells. GFP–sadA localized to the cell surface, confirming several computer predictions that sadA is a membrane protein and supporting the idea that sadA is a plasma membrane adhesion protein.

SadA mutants have a complex phenotype

In addition to the strong adhesion deficiency, sadA mutants show an interesting cytokinesis defect. In mutant cells of wild-type size, we often observed failed divisions by imaging live cells. Typically, the mutant cells tried to pull apart, but eventually "snapped back" together, suggesting that a lack of traction force might be responsible for this cytokinesis failure (Fig. 6; Videos 1 and 2). These cells completed nuclear divisions, becoming multinucleate. Often, multinucleate cells (typically with ten or fewer nuclei) were observed to divide into many mononucleate daughter cells simultaneously, despite being completely detached and floating (Video 1). This also manifested itself in a higher growth rate. For sadA-null mutants, it seems to make no difference whether they are grown in stationary plates or in shaking culture. Under both conditions, they efficiently grow without significant substrate adhesion. This is very different from cytoskeletal mutants, e.g., myosin II mutants, which fail to divide in suspension and become multinucleate, while dividing normally when grown on a surface (Manstein et al., 1989; Chen et al., 1994). In contrast, once sadA cells become large enough, they divide very efficiently, independent of traction forces, suggesting that they perform myosin-dependant cytokinesis A efficiently, but myosin-independent cytokinesis B very poorly (Zang et al., 1997). The complex phenotype of sadA mutants, including defective phagocytosis and cytokinesis, has been observed previously in chemically induced adhesion mutants, although the identities of the genes responsible were never determined (Waddell et al., 1987). In several regards, the sadA phenotypes resemble those of talin-null mutants. In *Dictyostelium*, talin has been shown to colocalize with F-actin in polarized cells (Kreitmeier et al., 1995). Talin-null cells, like sadA-null cells, have both an adhesion and phagocytosis defect and are slightly impaired in cytokinesis (Niewohner et al., 1997). Although the phagocytosis and adhesion phenotypes appear stronger in sadA mutants than in talin mutants, the parallels between the two mutants are significant. Because talin connects membrane proteins to the cytoskeleton, and sadA seems to participate in organizing F-actin (Fig. 5), an intriguing possibility is that talin and sadA act in a common pathway responsible for both particle and substrate adhesion (see model, Fig. 10).

Adhesion and phagocytosis

There is a strong correlation between adhesion and phagocytosis. A number of mutants defective in both functions have been described (e.g., phg1, talin, and myosin VII) (Waddell et al., 1987; Jung et al., 1996; Niewohner et al., 1997; Cornillon et al., 2000; Tuxworth et al., 2001). This may reflect a requirement for particle adhesion as a prerequisite for efficient phagocytosis. The observation of a severe phagocytosis defect in a mutant isolated for loss of substrate adhesion

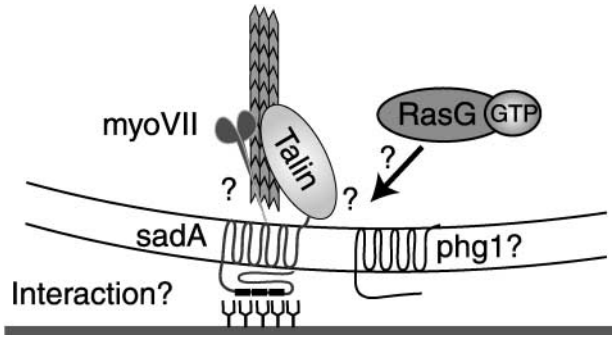

Figure 10. **Model summarizing the *Dictyostelium* proteins that are known to play a role in substrate adhesion.** Myosin VII -, phg1-, and talin-null mutants all display an adhesion defect. Phg1 is a nine-transmembrane molecule involved in particle adhesion. While talin is known to link integrin to the cytoskeleton in higher organisms, it might link an adhesion receptor like sadA to the cytoskeleton in *Dictyostelium*. Myosin VII might be involved in the organization of molecules of the adhesion machinery. Activated rasG may regulate and activate a putative adhesion complex. SadA is the first putative adhesion receptor that is absolutely required for substrate adhesion in growth medium. It is possible that sadA, via its intracellular domain(s), is linked to the cytoskeleton. The extracellular EGF-like repeats (depicted in three black boxes) are prime candidates that may bind to external molecules, which may allow the cells to attach and spread.

strongly supports this idea. During phagocytosis, GFP–sadA localized throughout the cortex, including the phagocytic cups, placing it at the correct location to participate in both substrate and particle adhesion. Phagocytosis of beads is completely abolished in sadA-null mutants. This is different from several myosin I mutants, which have been reported to play a minor role in phagocytosis (Jung et al., 1996; Schwarz et al., 2000). The defect is also stronger than that of myosin VII–null mutants, where phagocytosis of beads was reduced by 80% (Fig. 7 B; Titus, 1999). Interestingly, subsequent motility studies on the myosin VII mutants showed defective substrate adhesion in the leading edge (Tuxworth et al., 2001). Although myosin VII might be involved in the organization or transport of adhesion molecules, this function may overlap with those of other myosins. In contrast, the deletion of the major adhesion receptor would have a more deleterious impact on functions involving adhesion. The almost complete loss of substrate adhesion in sadA mutants, together with its membrane localization, makes sadA an excellent candidate for the primary substrate adhesion receptor in vegetative *Dictyostelium* cells.

SadA plays a major role in vegetative cells, but not during development

There are two other candidates for substrate adhesion receptors in *Dictyostelium*. Phg1, discovered in a screen for phagocytosis mutants, showed deficient substrate adhesion under shear stress conditions. Decreased adhesiveness was also observed by scanning electron microscopy, which showed that phg1 cells were detached locally and not as spread as wild type (Cornillon et al., 2000). Phg1 is a putative nine-transmembrane protein with no similarity to sadA. Although the phagocytosis defects might be comparable in phg1 and sadA mutants, the adhesion defect seems to be considerably milder in phg1 mutants than in sadA mutants. After prolonged culture in HL-5, phg1 mutants were reported to adhere, albeit not as tightly as wild type. Prolonged culture of sadA mutants, however, does not increase their ability to adhere to plastic. The second adhesion receptor candidate is a 130-kd surface glycoprotein, altered in chemically induced phagocytosis mutants (Vogel et al., 1980; Chia, 1996). Very little is known about this molecule. Our insertional mutagenesis screen suggests that there are numerous genes required for substrate adhesion. It will be instructive to characterize the collection of molecules involved in adhesion and their interactions.

Our results suggest that sadA, and thus adhesion, plays an important role in cell motility. The observation that sadA mutants actually migrate with increased speed suggests that sadA-mediated adhesion acts as a brake on cell movement (Fig. 8). It is important to note, however, that the sadA mutation affects migration only in vegetative amoebae, not in developing cells. This is consistent with the observation that F-actin localization is abnormal in vegetative cells, but not in cells starved for 4 h, which showed normal actin organization. Because sadA transcript levels decrease greatly after 4 h starvation, it seems likely that sadA's substrate adhesion function is assumed by other molecule(s) during development.

Extracellular EGF-like repeats suggest that sadA is an adhesion receptor

About 120 residues in the predicted extracellular domain of sadA show strong sequence similarity to tenascin A. This similarity is restricted to three EGF-like domains, which are similar to tenascin's 13 EGF-like repeats. Tenascins are a family of extracellular matrix proteins involved in adhesion, wound healing, and tumorgenesis and metastasis (for review see Jones and Jones, 2000). SadA's EGF repeats, especially the first repeat, are also very similar to a region in the extracellular domain of β integrin. To date, integrin homologues have not been identified in *Dictyostelium*. Integrins are major adhesion receptors in metazoan cells, anchored by one transmembrane domain. This sequence similarity and the presence of EGF-like repeats, together with the loss of substrate attachment in sadA mutants, support the hypothesis that sadA is an adhesion receptor perhaps capable of binding as yet unidentified extracellular ligands. Although sadA could also function in the regulation of adhesion, its cortical localization and the presence of external EGF-like domains favor a role as an adhesion protein. Upon ligand binding, the receptor might interact, via its cytoplasmic portion, with adaptor molecules, such as talin, that provide a link to the actin cytoskeleton. This idea is also supported by the aberrant F-actin organization in vegetative sadA mutant cells. Other molecules likely to be involved in a putative adhesion complex, or its regulation, might include molecular motors such as myosin VII and regulatory proteins such as rasG (Tuxworth et al., 1997; Chen and Katz, 2000; Tuxworth et al., 2001). Fig. 10 shows a model for how these gene products might interact. Our genetic screen has identified several other possible members or regulators of the adhesion system.

EGF-like repeats are generally located in the extracellular domain of membrane or extracellular proteins. Appropri-

ately, the repeats in sadA are located in a region predicted to be extracellular. So far, EGF-like domains have been mostly identified in animal proteins, however, they have been discovered outside the animal kingdom in *Arabidopsis* (Kohorn et al., 1992), in surface proteins of the malaria parasite *Plasmodium* (Kaslow et al., 1988), and in the spore coat protein sp60 of *Dictyostelium* (Widdowson et al., 1990). Despite their apparent abundance, the significance of EGF-like repeats remains elusive. In the neurogenic factor notch, several of its 36 EGF repeats were found to interact with ligands delta and serrate (Lawrence et al., 2000), but the functions of the ligands' own EGF-like repeats are unknown. In tenascin A, EGF-like repeats seem to have adhesion-stimulating activities, but the activity might be counteracted by other domains in the protein, complicating the clear analysis of EGF repeat function (Fischer et al., 1997). Therefore, the presence of EGF-like repeats in an adhesion molecule of a simple organism marks an important observation. Interestingly, the recent analysis of the first, fully sequenced *Dictyostelium* chromosome (representing 25% of the genome) revealed that EGF-like domains are relatively more abundant in *Dictyostelium* than in any other sequenced organism, including humans (Glöckner et al., 2002). It is an interesting possibility that the molecules that appear to take over sadA's adhesion function in development could well be among these other EGF domain–containing proteins. With many tools in hand for genetic, molecular, and biochemical analyses, future studies of the sadA molecule in *Dictyostelium* might not only provide clues about the protein itself but also for the understanding of EGF repeat function(s) in general.

In conclusion, the application of a straightforward selection regime to a population of *Dictyostelium* cells mutagenized by insertional mutagenesis led to the isolation of several *Dictyostelium* substrate adhesion mutants. One of these, sadA, appears to be a novel adhesion molecule, required for cell substrate adhesion, phagocytosis, normal F-actin organization, and efficient cytokinesis. SadA is likely to interact with other molecules, both inside and outside of the cell. Although talin or myosin VII are potential intracellular partners, extracellular candidates remain a mystery. However, the external EGF-like repeats not only make such an interaction likely, they also provide excellent targets for further exploration. The ongoing investigation of sadA and other mutants identified in our genetic screen should lead to a better understanding of adhesion in crawling cells.

Materials and methods

REMI screen and other transformations

Transformations were modified from Pang et al. (1999). In brief, a Bio-Rad Laboratories gene pulser set to 0.85 kV/25 μF was used to electroporate 10 μg BamHI-linearized pUCΔBamBsr (Adachi et al., 1994) together with 10 U DpnII enzyme (NEB) into 7×10^6 wild-type (AX3) cells. The volume was 100 μl and the cuvette gap size was 1 mm, resulting in a time constant of 0.7 ms. Cells were incubated in HL-5 in a Petri dish to recover overnight before 10 μg/ml blasticidin (ICN Biomedicals) was added. After 3–5 d, floating (nonattached) cells were transferred to a new dish. This process was repeated for 2–4 wk, medium was replaced approximately every 5 d. Clones of the enriched nonattached cells were isolated by limiting dilution in 96-well plates. Other constructs were transformed using the same electroporation settings. psadA–GFP-transformed cells were selected on a bacterial lawn (Fey et al., 1995). Cells were spread with *Escherichia coli* B/r-1 on LPB plates (0.1% lactose, 0.1% bacto peptone, 19 mM Na_2HPO_4*$7H_2O$, 30 mM KH_2PO_4, 2% agar) containing 20 μg/ml G418 (Mediatech Inc.).

Isolation and sequencing of genomic flanking regions

Plasmid rescue to clone sequences flanking the plasmid insertion was performed as previously described (Fey and Cox, 1999). In brief, 300 ng genomic DNA was digested with EcoRI and ligated at a DNA concentration of 1 ng/μl, with 1.3 U/μl T4 ligase (NEB) at 16°C for 24 h. The ligation products were ethanol precipitated, resuspended in 5 μl water, and electroporated into 50 μl *E. coli* DH10B. The cloned flanking sequences were sequenced automatically using custom primers and dye terminator chemistry (PerkinElmer). The resulting sequences were subjected to a blast search against the *Dictyostelium* genomic DNA sequence database. In the case of mutant 3IIG11, an ~300-bp flanking sequence matched a portion of contig 15235. The sequence information obtained from the database and the plasmid insertion site were then verified by PCR using wild-type and mutant genomic DNA.

Cloning of the sadA cDNA and plasmid constructs

For all experiments, restriction enzymes came either from NEB or from Roche Biochemicals. All PCR reactions were performed using High Fidelity polymerase (Roche Biochemicals). The 5′ 2,200 bp of the cDNA were amplified by PCR from a cDNA library (provided by D. Robinson, Johns Hopkins University, Baltimore, MD; Robinson and Spudich, 2000) using primers AGAGGATCCAAAAAAAAAATGAAATCCCAAAAAATAGG and GGAATGATGATTCTATAGTCATG. The amplified DNA was digested with BamHI and HindIII, and the resulting 1,750-bp fragment was cloned into BamHI/HindIII-cut pBluescript KS+ (Stratagene) (pKS5′sadA). To clone the 3′ end, the cDNA library was screened with two cDNA probes, derived from both ends of the known 1,750-bp fragment. Double positive clones were sequenced, revealing a 500-bp stretch of additional coding sequence.

The knock-out construct was made by amplifying a 950-bp 5′ sequence by PCR with primers GAGTATCGATAAACATTTCATTTCTGTAATACG and GAGTGGATCCACCTGAACTTCTTAAGTTTGC. A 600-bp 3′ sequence was amplified using primers CACAGAATTCTAAACGTGCTAAAGATTATGCAG and CACAATCGATGGAATGATGATTCTATAGTCATG. The PCR fragments were digested with ClaI/BamHI or EcoRI/ClaI, respectively, and cloned into pUCΔBamBsr, which had been digested with BamHI/EcoRI. Prior to transformation, the resulting psadAKO was linearized with ClaI and blunt ended using Klenow enzyme. As confirmed by PCR, insertion of the plasmid into the genome by homologous recombination resulted in the deletion of a 1-kb coding sequence.

To make psadA–GFP, a 1,600-bp 5′ cDNA fragment was isolated from pKS5′sadA by digestion with BamHI and SphI. A 1,340-bp 3′ fragment was amplified by PCR from the cDNA library with primers GTGTGAAGTTGATGGACTTTGC and AGAGGATCCTTTCTTAGATAAATCGATTTCACC and was subsequently digested with SphI/BamHI. Both the 5′ and 3′ fragments were cloned into BamHI-digested pA15GFP to produce an in-frame COOH-terminal GFP fusion.

Northern blot

Total cellular RNA of vegetative wild-type and mutant cells, or of wild-type cells at the 2-, 4-, 6-, 8-, and 16-h starvation stage, was prepared using a guanidine thiocyanate CsCl gradient (Davis et al., 1986). Hybridizations were performed using standard procedures (Sambrook et al., 1989) in a solution containing 50% formamide, 5× Denhardt's, 5× SSC, 0.5% SDS, 100 μg/ml salmon sperm DNA at 42°C. After hybridization, blots were washed twice with 2× SSC/0.5% SDS and twice with 0.2× SSC/0.5% SDS at 65°C before exposure to x-ray film. Probes contained 500 bp of the sadA cDNA and were labeled with a random prime labeling kit (Stratagene).

Attachment assays

For attachment assays, cells were plated at 10^5 per ml HL-5 and incubated overnight at room temperature. The next day, dishes were shaken at speeds varying from 10 to 75 rpm. After 1 h, cells that could not attach were pipetted off the plate, concentrated by centrifugation if necessary, and counted in a Neubauer counting chamber. Control plates that were not shaken were used to take the total cell count or the 0 rpm data.

Determination of growth rates

Growth rates were determined by inoculating 10^5 cells/ml into 10 ml HL-5. Cells were shaken at 200 rpm, 20°C for a total of 72 h. Samples were counted every 24 h.

Phagocytosis assays and flow cytometry

The rate of phagocytosis was measured by analyzing the intensity of green fluorescence emanating from beads internalized over the course of 9 min using an assay modified from the protocol published by Tuxworth et al. (2001). Cells were grown in HL-5 to a subconfluent density and washed once with SB (16.6 mM Na/KPO_4, pH 6.4, and 1 mM $MgCl_2$). 10^6 cells were resuspended in 900 μl SB, placed in a well of a 24-well plate (Falcon 3047), and rotated at 175 rpm for 1 h. Yellow green carboxylate microspheres of 1.0 μm diameter (Polysciences) were resuspended in water and 100 μl was added to the cells to produce a final concentration of 2×10^8 beads/ml. For each time point, a 75-μl aliquot was taken from the well and added to 1.0 ml of ice-cold fixative (1.5% formaldehyde in methanol). To remove unincorporated beads, the fixed samples were pelleted through a PEG8000 solution, resuspended in SB, and the mean fluorescence of 1,000 cells was quantified using a FACScan® flow cytometer (excitation = 488 nm, emission = FL1-H, detector voltage set at 350; Becton Dickinson).

To physically sort cells expressing the sadA–GFP fusion protein based on GFP fluorescence, cells were resuspended in SB at 10^7 cells/ml and processed using a FACSVantage® SE flow cytometer (Becton Dickinson) configured with turbosort. The cytometer used an Innova 304 water-cooled laser with an output of 100 mW using an excitation wavelength of 488 nm and a BP530/30 emission filter. Cells were sorted into two populations: the brightest 10% and the dimmest 10%. The phagocytosis ability was measured immediately after sorting.

To localize sadA in phagocytic cups, sadA–GFP cells were allowed to adhere to a coverslip before heat-killed yeast was added. After 15 min, unattached yeast was washed off in phosphate buffer, followed by fixation in a solution of picric acid and formaldehyde as described in detail by Maniak et al. (1995). Fixed cells were visualized by confocal microscopy (Bio-Rad Laboratories) using a 60× objective.

Fixation, F-actin, and DAPI staining

For actin staining, cells were allowed to settle for 15 min in phosphate buffer containing Ca and Mg (5 mM Na_2HPO_4, 5 mM KH_2HPO_4, 1 mM $CaCl_2$, 2 mM $MgCl_2$). Subsequently, the cells were fixed in 0.85% formaldehyde in methanol at −20°C for 5 min and incubated with Alexa®568-phalloidin (Molecular Probes) according to the manufacturer's instruction. For the 4-h developmental stage, cells were starved in the same buffer for 4 h before fixation. The actin profiles were created using NIH Image 1.62 software.

For the DAPI staining, mutant cells in phosphate buffer (5 mM Na_2HPO_4, 5 mM KH_2HPO_4) were allowed to settle in a humid chamber for 30 min and then overlaid with a thin agarose sheet (Fukui et al., 1987) before fixation to flatten the cells. Other cells were allowed to adhere and were overlaid with agarose, after which all coverslips were dipped into ice-cold anhydrous methanol and fixed for 5 min at −20°C. DAPI was used at 20 μg/ml in H_2O, and incubation was for 5 min at room temperature.

Fluorescence and live cell microscopy

The microscope used was a ZEISS Axiovert S100-TV inverted fluorescent microscope. Live cells were imaged while growing in HL-5 in a glass-bottom Petri dish using a 40× objective. Images were captured with a Micromax cooled CCD camera (Princeton Instruments) driven by Metamorph 4.5 software (Universal Imaging Corp.). Cell migration was tracked using the same software.

Online supplemental material

The online supplemental material is available online at http://www.jcb.org/cgi/content/full/jcb.200206067/DC1. All images for the videos were taken with a ZEISS Axiovert S100-TV inverted microscope. For Videos 1 and 2, live vegetative cells were observed while growing in HL-5 in a glass-bottom dish. An image was taken every 20 s using a 40× objective. For Videos 3 and 4, streaming cells were observed after they had been washed three times with phosphate buffer containing Ca and Mg. 30 min after plating in the same buffer, images were taken every 3 min for a total of 7 h using a 10× objective.

We would like to thank Lina Nayak for carrying out the adhesion assays, Doug Robinson for providing the cDNA library, Teng-Leong Chew for his help with microscopy, and Shuo Ma for critical reading of the manuscript.

This work was funded by National Institutes of Health grant GM39264 to R.L. Chisholm. The GenBank/EMBL/DDBJ accession no. for sadA is AY178767.

Submitted: 14 June 2002
Revised: 8 November 2002
Accepted: 8 November 2002

References

Adachi, H., T. Hasebe, K. Yoshinaga, T. Ohta, and K. Sutoh. 1994. Isolation of *Dictyostelium* discoideum cytokinesis mutants by restriction enzyme-mediated integration of the blasticidin S resistance marker. *Biochem. Biophys. Res. Commun.* 205:1808–1814.

Aguado-Velasco, C., and M.S. Bretscher. 1999. Circulation of the plasma membrane in *Dictyostelium. Mol. Biol. Cell.* 10:4419–4427.

Brar, S., and C. Siu. 1993. Characterization of the cell adhesion molecule gp24 in *Dictyostelium discoideum*. Mediation of cell-cell adhesion via a Ca(2+)-dependent mechanism. *J. Biol. Chem.* 268:24902–24909.

Burridge, K., and L. Connell. 1983. Talin: a cytoskeletal component concentrated in adhesion plaques and other sites of actin-membrane interaction. *Cell Motil.* 3:405–417.

Burridge, K., and P. Mangeat. 1984. An interaction between vinculin and talin. *Nature.* 308:744–746.

Chen, C.F., and E.R. Katz. 2000. Mediation of cell-substratum adhesion by RasG in *Dictyostelium. J. Cell. Biochem.* 79:139–149.

Chen, P.X., B.D. Ostrow, S.R. Tafuri, and R.L. Chisholm. 1994. Targeted disruption of the *Dictyostelium* RMLC gene produces cells defective in cytokinesis and development. *J. Cell Biol.* 127:1933–1944.

Chia, C.P. 1996. A 13O-kDa plasma membrane glycoprotein involved in *Dictyostelium* phagocytosis. *Exp. Cell Res.* 227:182–189.

Cornillon, S., E. Pech, M. Benghezal, K. Ravanel, E. Gaynor, F. Letourneur, F. Bruckert, and P. Cosson. 2000. Phg1p is a nine-transmembrane protein superfamily member involved in *Dictyostelium* adhesion and phagocytosis. *J. Biol. Chem.* 275:34287–34292.

Davis, L., M. Dibner, and J. Battey. 1986. Methods in Molecular Biology. Elsevier Science Publishing Co. Inc., New York. 388 pp.

Fey, P., and E.C. Cox. 1999. Cortexillin I is required for development in *Polysphondylium. Dev. Biol.* 212:414–424.

Fey, P., K. Compton, and E.C. Cox. 1995. Green fluorescent protein production in the cellular slime molds *Polysphondylium pallidum* and *Dictyostelium discoideum*. *Gene.* 165:127–130.

Fischer, D., M. Brown-Ludi, T. Schulthess, and R. Chiquet-Ehrismann. 1997. Concerted action of tenascin-C domains in cell adhesion, anti-adhesion and promotion of neurite outgrowth. *J. Cell Sci.* 110:1513–1522.

Friedl, P., S. Borgmann, and E. Bröcker. 2001. Amoeboid leukocyte crawling through extracellular matrix: lessons from the *Dictyostelium* paradigm of amoeboid movement. *J. Leukoc. Biol.* 70:491–509.

Fukui, Y., S. Yumura, and T. Yumura. 1987. Agar-overlay immunofluorescence: high-resolution studies of cytoskeletal components and their changes during chemotaxis. *Methods Cell Biol.* 28:347–356.

Gao, E.N., P. Shier, and C.H. Siu. 1992. Purification and partial characterization of a cell adhesion molecule (gp150) involved in postaggregation stage cell-cell binding in *Dictyostelium discoideum. J. Biol. Chem.* 267:9409–9415.

Glöckner, G., L. Eichinger, K. Szafranski, J. Pachebat, A. Bankier, P. Dear, R. Lehmann, C. Baumgart, G. Parra, J. Abril, et al. 2002. Sequence and analysis of chromosome 2 of *Dictyostelium discoideum. Nature.* 418:79–85.

Horwitz, A., K. Duggan, C. Buck, M. Beckerle, and K. Burridge. 1986. Interaction of plasma membrane fibronectin receptor with talin–a transmembrane linkage. *Nature.* 320:531–533.

Jones, F., and P. Jones. 2000. The tenascin family of ECM glycoproteins: structure, function, and regulation during embryonic development and tissue remodeling. *Dev. Dyn.* 218:235–259.

Jung, G., X.F. Wu, and J.A. Hammer. 1996. *Dictyostelium* mutants lacking multiple classic myosin I isoforms reveal combinations of shared and distinct functions. *J. Cell Biol.* 133:305–323.

Kaslow, D., I. Quakyi, C. Syin, M. Raum, D. Keister, J. Coligan, T. McCutchan, and L. Miller. 1988. A vaccine candidate from the sexual stage of human malaria that contains EGF-like domains. *Nature.* 333:74–76.

Knezevic, I., T. Leisner, and S. Lam. 1996. Direct binding of the platelet integrin αIIbβ3 (GPIIb-IIIa) to talin. Evidence that interaction is mediated through the cytoplasmic domains of both αIIb and β3. *J. Biol. Chem.* 271:16416–16421.

Kohorn, B., S. Lane, and T.A. Smith. 1992. An *Arabidopsis* serine/threonine kinase homologue with an epidermal growth factor repeat selected in yeast for its specificity for a thylakoid membrane protein. *Proc. Natl. Acad. Sci. USA.* 89: 10989–10992.

Kreitmeier, M., G. Gerisch, C. Heizer, and A. Muller-Taubenberger. 1995. A talin homologue of *Dictyostelium* rapidly assembles at the leading edge of cells in response to chemoattractant. *J. Cell Biol.* 129:179–188.

Krogh, A., B. Larsson, G. von Heijne, and E. Sonnhammer. 2001. Predicting transmembrane protein topology with a hidden Markov model: application

to complete genomes. *J. Mol. Biol.* 305:567–580.

Kuspa, A., and W.F. Loomis. 1992. Tagging developmental genes in *Dictyostelium* by restriction enzyme-mediated integration of plasmid DNA. *Proc. Natl. Acad. Sci. USA.* 89:8803–8807.

Lawrence, N., T. Klein, K. Brennan, and A. Martinez Arias. 2000. Structural requirements for notch signalling with delta and serrate during the development and patterning of the wing disc of *Drosophila*. *Development.* 127: 3185–3195.

Maniak, M., R. Rauchenberger, R. Albrecht, J. Murphy, and G. Gerisch. 1995. Coronin involved in phagocytosis: dynamics of particle-induced relocalization visualized by a green fluorescent protein tag. *Cell.* 83:915–924.

Manstein, D.J., M.A. Titus, A. De Lozanne, and J.A. Spudich. 1989. Gene replacement in *Dictyostelium*: generation of myosin null mutants. *EMBO J.* 8:923–932.

Moller, S., M. Croning, and R. Apweiler. 2001. Evaluation of methods for the prediction of membrane spanning regions. *Bioinformatics.* 17:646–653.

Moulder, G., M. Huang, R. Waterston, and R. Barstead. 1996. Talin requires β-integrin, but not vinculin, for its assembly into focal adhesion-like structures in the nematode *Caenorhabditis elegans*. *Mol. Biol. Cell.* 7:1181–1193.

Muguruma, M., S. Matsumura, and T. Fukazawa. 1990. Direct interactions between talin and actin. *Biochem Biophys Res Commun*. 171:1217–1223.

Niewohner, J., I. Weber, M. Maniak, A. Muller-Taubenberger, and G. Gerisch. 1997. Talin-null cells of *Dictyostelium* are strongly defective in adhesion to particle and substrate surfaces and slightly impaired in cytokinesis. *J. Cell Biol.* 138:349–361.

Pang, K.M., M.A. Lynes, and D.A. Knecht. 1999. Variables controlling the expression level of exogenous genes in *Dictyostelium. Plasmid.* 41:187–197.

Ponte, E., E. Bracco, J. Faix, and S. Bozzaro. 1998. Detection of subtle phenotypes: the case of the cell adhesion molecule csA in *Dictyostelium. Proc. Natl. Acad. Sci. USA.* 95:9360–9365.

Robinson, D.N., and J.A. Spudich. 2000. Dynacortin, a genetic link between equatorial contractility and global shape control discovered by library complementation of a *Dictyostelium discoideum* cytokinesis mutant. *J. Cell Biol.* 150:823–838.

Sambrook, J., E.F. Fritsch, and T. Maniatis. 1989. Molecular Cloning. A Laboratory Manual. Second edition. Cold Spring Harbor Laboratory, Cold Spring Harbor, NY.

Schwarz, E.C., E.M. Neuhaus, C. Kistler, A.W. Henkel, and T. Soldati. 2000. *Dictyostelium* myosin IK is involved in the maintenance of cortical tension and affects motility and phagocytosis. *J. Cell Sci.* 113:621–633.

Siu, C., T. Lam, and A. Choi. 1985. Inhibition of cell-cell binding at the aggregation stage of *Dictyostelium discoideum* development by monoclonal antibodies directed against an 80,000-dalton surface glycoprotein. *J. Biol. Chem.* 260:16030–16036.

Titus, M.A. 1999. A class VII unconventional myosin is required for phagocytosis. *Curr. Biol.* 9:1297–1303.

Tuxworth, R.I., J.L. Cheetham, L.M. Machesky, G.B. Spiegelmann, G. Weeks, and R.H. Insall. 1997. *Dictyostelium* RasG is required for normal motility and cytokinesis, but not growth. *J. Cell Biol.* 138:605–614.

Tuxworth, R.I., I. Weber, D. Wessels, G.C. Addicks, D.R. Soll, G. Gerisch, and M.A. Titus. 2001. A role for myosin VII in dynamic cell adhesion. *Curr. Biol.* 11:318–329.

Varney, R., E. Casademunt, H. Ho, C. Petty, J. Dolman, and D. Blumberg. 2002. A novel *Dictyostelium* gene encoding multiple repeats of adhesion inhibitor-like domains has effects on cell-cell and cell-substrate adhesion. *Dev. Biol.* 243:226–248.

Vogel, G., L. Thilo, H. Schwarz, and R. Steinhart. 1980. Mechanism of phagocytosis in *Dictyostelium discoideum*: phagocytosis is mediated by different recognition sites as disclosed by mutants with altered phagocytotic properties. *J. Cell Biol.* 86:456–465.

Waddell, D.R., K. Duffy, and G. Vogel. 1987. Cytokinesis is defective in *Dictyostelium* mutants with altered phagocytic recognition, adhesion, and vegetative cell cohesion properties. *J. Cell Biol.* 105:2293–2300.

Wang, J., L. Hou, D. Awrey, W.F. Loomis, R.A. Firtel, and C.H. Siu. 2000. The membrane glycoprotein gp150 is encoded by the lacC gene and mediates cell-cell adhesion by heterophilic binding during *Dictyostelium* development. *Dev. Biol.* 227:734–745.

Widdowson, D.C.C., J.A. Proffitt, P.S. Jagger, A.J. Richards, and B.D. Hames. 1990. Developmental expression and characterization of the gene encoding spore coat protein sp60 in *Dictyostelium discoideum*. *Mol. Microbiol.* 4:951–960.

Wong, E.F.S., S.K. Brar, H. Sesaki, C.Z. Yang, and C.H. Siu. 1996. Molecular cloning and characterization of DdCAD-1, a Ca2+- dependent cell-cell adhesion molecule, in *Dictyostelium* discoideum. *J. Biol. Chem.* 271:16399–16408.

Zang, J.H., G. Cavet, J.H. Sabry, P. Wagner, S.L. Moores, and J.A. Spudich. 1997. On the role of myosin-II in cytokinesis: division of *Dictyostelium* cells under adhesive and nonadhesive conditions. *Mol. Biol. Cell.* 8:2617–2629.